Wavelength switching in multi-cavity laser diodes

S. M. K. Thiyagarajan, A. P. Kanjamala, and A. F. J. Levi[a)]
Electrical Engineering Department, University of Southern California, University Park, DRB 118, Los Angeles, California 90089-1111

(Received 21 October 1997; accepted for publication 6 May 1998)

We study experimentally and numerically electrical and optical methods to switch the lasing wavelength in a linear multi-cavity laser. The electrical method uses radio frequency modulation of the gain region to modify effective optical loss at a well-defined wavelength. The optical method uses injection of lasing light to modify effective photon lifetime at the injection wave-length. Short transient switching times corresponding to less than two photon-cavity round-trips are observed using both methods. However, this occurs for small spectral separation between lasing wavelengths, a less effective mode suppression ratio, and an asymmetry in switching time to and from a given lasing wavelength. The maximum wavelength switching speed is determined by the net optical gain and the initial number of photons in each cavity mode. © *1998 American Institute of Physics.* [S0021-8979(98)02916-8]

I. INTRODUCTION

Interpreting observations of transient effects in short single external-cavity semiconductor lasers[1] has been hampered by the inherent complexity of coupling between carriers and photons. To circumvent these difficulties, O'Gorman *et al.*[2] studied photon-cavity formation in long external cavity semiconductor lasers by decoupling the effects of transient carrier dynamics from photon intensity buildup. Huhse and co-workers[3] then showed that lasing wavelength could be switched electrically in gain-switched self-seeded external-cavity lasers. Kanjamala *et al.*[4] independently reported on the transient dynamics of wavelength switching using radio frequency (rf) electrical input for multi-cavity mode-locked laser diodes.

Given the above background of experimental studies, the purpose of this article is to establish a model which describes the transients of rf induced wavelength switching. In addition, we report on experiments and calculations for all-optical wavelength switching in multi-cavity lasers.

A multi-cavity laser is a semiconductor laser diode with an anti-reflection (AR) coating on one facet subject to optical feedback from a series of spatially separated Bragg gratings embedded in a single-mode fiber (SMF). Figure 1 is a schematic of the two-cavity situation. The lasing wavelength prior to switching is λ_{HOT} and the corresponding photon-cavity is the hot cavity.[4] The nonlasing wavelength and the corresponding cavity are the cold wavelength, λ_{COLD}, and cold cavity, respectively. It is to be noted that λ_{HOT} can either be longer or shorter than λ_{COLD}. In Sec. II, we describe the experimental arrangement, experimental results, and our modeling of wavelength switching using an rf signal. In Sec. III, we describe and model an alternate all-optical technique of wavelength switching and report the experimental results. Section IV summarizes the results of this work.

a)Electronic mail: alevi@usc.edu

II. WAVELENGTH SWITCHING USING rf MODULATION

For frequencies less than approximately 30 GHz, the small-signal rf response of a typical as-cleaved edge-emitting semiconductor laser diode is dominated by the geometric mean of the stimulated carrier lifetime and photon lifetime. The photon-cavity round-trip time does not play a role because typical round-trip times are only a few ps. However, in an external-cavity laser the photon round-trip time can be increased so that it is comparable or larger than the geometric mean of the stimulated carrier lifetime and photon lifetime. In this regime, resonance peaks are observed in the rf spectrum corresponding to approximately integer multiples of the inverse of the photon round-trip time (defined as the cavity frequency).

The rf response is understood as a change in the effective gain/loss experienced by photons which are modulated at that rf frequency. The effective loss is $K_{\text{eff}}(f_{\text{RF}},\omega_0)$, where f_{RF} is the rf frequency and ω_0 the optical frequency of the mode. Consider a laser with competition between various optical modes. The dominant steady-state lasing mode will be the one with the larger gain and a smaller loss. However, by modulation of laser injection current with a rf frequency it is possible to alter the effective loss of each mode. Hence, one may change a steady-state nonlasing mode into a lasing mode with rf modulation f_{RF} and vice versa. This additional degree of freedom enables one to independently tailor $K_{\text{eff}}(f_{\text{RF}},\omega_0)$ for the different modes of a multi-cavity laser. This is the principle involved in wavelength switching of a multi-cavity laser using a rf signal.

A. Experimental arrangement and results

An AR coated multiple quantum well semiconductor laser diode with optical emission at $\lambda=1.3$ μm is used. The as-cleaved 300 μm long device[5] has a threshold current $I_{\text{th}}=6$ mA which after AR coating increases to 22 mA. Optical emission from the AR coated side of the diode is coupled with an efficiency of 45% into a lensed single-mode

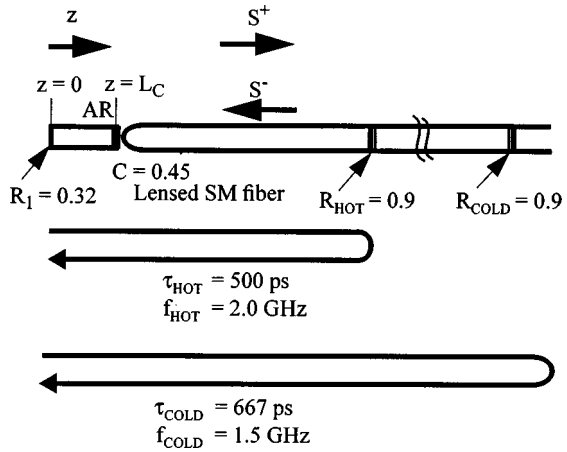

FIG. 1. Schematic of the multi-cavity laser used in our numerical study. The AR coated semiconductor laser is 300 μm long and has external cavities (cold and hot) defined by Bragg gratings at $\lambda_{HOT}=1.3165\,\mu$m and $\lambda_{COLD}=1.3125\,\mu$m with reflectivities of approximately 0.9 at both λ_{HOT} and λ_{COLD}. The coupling factor between the laser and the lensed single mode fiber is approximately 0.45. The non-AR coated facet has a reflectivity of 0.32 for both the wavelengths.

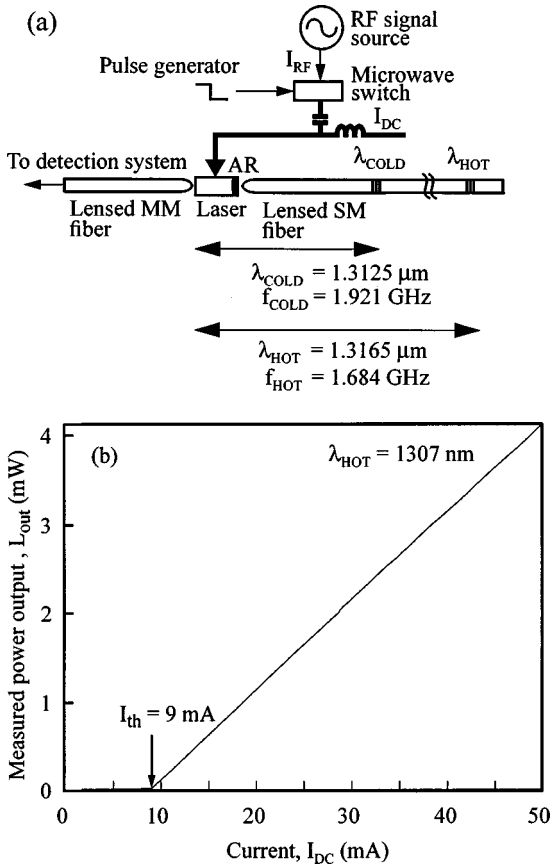

FIG. 2. (a) Experimental arrangement used to measure transient switching response after application of a large rf signal to the multi-cavity laser. Cavity length $L_{HOT}=5.9$ cm and $L_{COLD}=5.2$ cm. (b) The measured steady state L_{out}–I_{DC} characteristics.

fiber containing Bragg gratings. The SMF contains a series of ten Bragg gratings placed sequentially along its length. The Bragg gratings have center wavelengths ranging from 1307 to 1316 nm and a reflectivity of approximately 80%. However, relevant to this work are the cavities defined by gratings with -3 dB bandwidths of 0.3 nm and center wavelengths $\lambda_{HOT}=1316.5$ nm and $\lambda_{COLD}=1312.5$ nm with corresponding cavity lengths of $L_{COLD}=5.2$ cm and $L_{HOT}=5.9$ cm. The experimental arrangement used to study the transient response of the photons when switching wavelengths is shown in Fig. 2(a). The steady-state $L-I$ characteristic of the device shown in Fig. 2(b) exhibits a threshold current $I_{th}=9$ mA. Under steady-state bias conditions, lasing occurs at two of the Bragg grating defined wavelengths of $\lambda=1.3165\,\mu$m (λ_{HOT}) and $\lambda=1.3155\,\mu$m.

Initial transient response experiments are performed with the laser biased at $I_{DC}=30$ mA. A microwave switch is used to turn on the rf current applied to the laser. We define transient switching time as the time taken to reach 50% of the steady-state response. It is convenient to normalize all times to τ_{CAV}, the photon-cavity round-trip time. As seen in Fig. 3(a), the rf switch turns on in 0.5 ns corresponding to about one photon round-trip time in the external cavity. Figure 3(b) shows that it takes approximately 1.5 round-trip times after the rf signal at frequency $f_{HOT}=1.684$ GHz is applied to the laser to switch the lasing light output to $\lambda_{HOT}=1.3165\,\mu$m. The stimulated emission due to hot photons initially present in the cavity causes a very rapid turn-on, so that the measured value of the transient time is partially obscured by the response of the rf switch. However, as shown in Fig. 3(c), it takes eight photon round-trips for lasing to occur at λ_{COLD} after application of an rf signal of frequency $f_{COLD}=1.921$ GHz. Figure 3(c) also shows that it takes a few ($\sim$5–6) round-trip times for the lasing intensity at λ_{HOT} to be suppressed. Ringing in peak photon intensity shown in Figs. 3(b) and 3(c) arises from transient rf mismatch between microwave switch and laser diode (confirmed using electrical measurements). Figure 3(d) shows the time-averaged optical spectrum for three different cases: (i) When there is no rf signal applied to the laser, the device lases at λ_{HOT} (intensity peaks at other wavelengths are due to optical reflection from other Bragg gratings in the SMF). (ii) When a rf frequency f_{HOT} causes the device to switch to λ_{HOT}. The mode at $\lambda=1.3155\,\mu$m is suppressed since the cavity formed by this mode is not resonant (synchronized) with the rf signal at f_{HOT}. (iii) When a rf signal at frequency f_{COLD} is applied. Note the relative mode suppression ratio of greater than -30 dB.

The dependence of the transient time on steady-state bias, I_{DC}, as well as the rf signal power is shown in Fig. 4. The hot photon-cavity behaves differently above and below threshold. Above threshold, the hot photon-cavity reaches 50% of steady-state intensity in about 1.5 round-trip times independent of the applied rf signal power and the steady-state component of current bias I_{DC}. Below threshold, the transient switching time increases rapidly with decrease in either I_{DC} or decrease in rf signal power.

The transient switching time of the cold photon-cavity decreases with the increase in rf signal power both above and below threshold. Above threshold, the transient time for switching to λ_{COLD} is independent of I_{DC}. Below threshold, there is an increase in the transient time for switching to λ_{COLD} with decrease in I_{DC} at all rf signal power levels. As

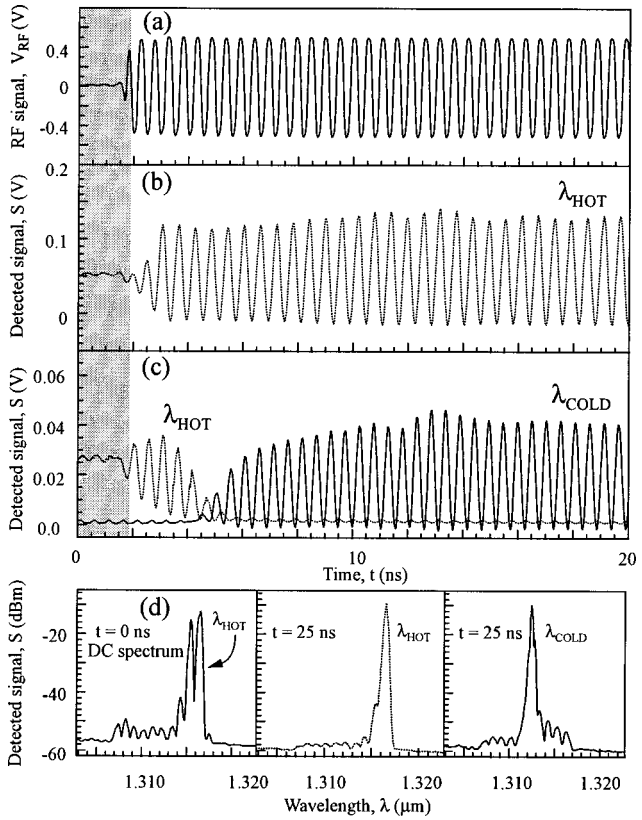

FIG. 3. Measured temporal response involved in optical wavelength switching: (a) rf signal applied to the laser; (b) transients involved switching to the hot wavelength when a 15 dB m rf signal at f_{HOT} is applied; (c) the buildup of power at λ_{COLD} and decay of power at λ_{HOT} when a 15 dB m rf signal at f_{COLD} is applied; (d) the time averaged optical spectrum with no rf, rf at f_{HOT}, and rf at f_{COLD}. The presence of intensity peaks at nonlasing wavelengths in the steady-state spectrum is due to reflection from other Bragg grating wavelengths in the fiber.

the laser is biased further below threshold, the transient switching time for λ_{HOT} tends towards that of λ_{COLD}. Before the rf signal is turned on, the laser cavity has very few hot photons when biased below threshold and this number decreases with a decrease in bias current. This suggests that the transient time to switch lasing wavelength and cavity length depends on the number of hot photons present in the cavity before the rf signal is turned on.

The interference between internal cavity modes (between the cleaved facet and the AR coated facet) and external cavity modes (between the fiber Bragg grating and the cleaved facet) leads to a detuning of lasing wavelength from the nominal center wavelength of the Bragg grating. A detailed description can be found elsewhere.[6] Lasing wavelength can be switched using a range of rf values. In our experiments the measured ~100 MHz rf bandwidth for stable wavelength switching is due to a spatial spread in photon reflection turning point in the Bragg grating.

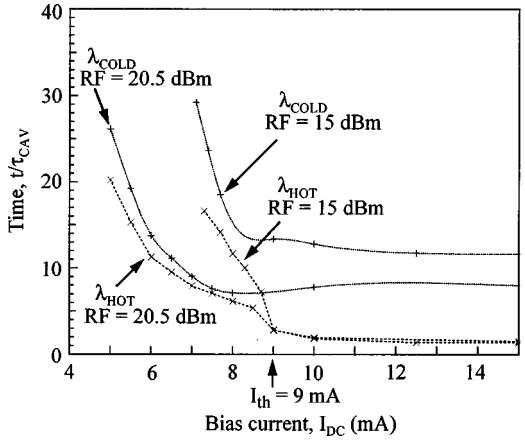

FIG. 4. The dependence of the transient switching time normalized to τ_{CAV} on the bias current, I_{DC}, and the applied rf power.

B. Modeling and numerical simulation

Spatially dependent photon density rate equations[7] are used to model the multi-cavity laser. In our model

$$\frac{d}{dt}S^+(\lambda_i)+\nu_g\frac{d}{dz}S^+(\lambda_i)=(G_i-\kappa_i)S^+(\lambda_i)+(\beta_i/2)R_{sp}, \tag{1}$$

$$\frac{d}{dt}S^-(\lambda_i)+(-\nu_g)\frac{d}{dz}S^-(\lambda_i) =(G_i-\kappa_i)S^-(\lambda_i)+(\beta_i/2)R_{sp}, \tag{2}$$

$$\frac{d}{dt}N(z,t)=\frac{I}{eV}-\sum_{i=\text{cold}}^{\text{hot}}G_i[S^+(\lambda_i)+S^-(\lambda_i)]-R_{sp}, \tag{3}$$

where S^+ is the photon density moving to the right, S^- is the photon density moving to the left, $N(z,t)$ is the electron carrier density, ν_g is the photon group velocity, $G_i(\kappa_i)$ is the optical gain (internal loss) at wavelength λ_i, R_{sp} is the spontaneous emission power, and β_i is the spontaneous emission factor. The boundary conditions are

$$S^+(0;t;\lambda)=R_1\times S^-(0;t;\lambda), \tag{4}$$

$$S^-(L_C;t;\lambda_{COLD})=R_{COLD}\times C^2 \times S^+[L_C;(t-\tau_{COLD});\lambda_{COLD}] \tag{5}$$

$$S^-(L_C;t;\lambda_{HOT})=R_{HOT}\times C^2\times S^+[L_C;(t-\tau_{HOT});\lambda_{HOT}], \tag{6}$$

where R_1 is the reflectivity (at both the wavelengths) of the non-AR coated facet, $\tau_{HOT(COLD)}$ is the round-trip time for the hot (cold) photons, C is the optical coupling factor between the semiconductor laser and the lensed single mode fiber, and $R_{HOT(COLD)}$ is the reflectivity of the grating at the corresponding wavelength. To simplify our analysis, the Bragg grating is assumed to have narrow bandwidth and we solve only the single-mode rate equations.

We model an AR-coated semiconductor laser of cavity length, $L_C=300\ \mu$m and external cavity lengths of L_{COLD} and L_{HOT}. The non-AR coated facet has a reflectivity $R_1=0.32$ at both the wavelengths and the reflectivity of the gratings at their respective center wavelengths is $R_{HOT}=R_{COLD}=0.90$. The coupling between the semiconductor laser and the lensed single mode fiber, $C=0.45$. Internal loss in the semiconductor laser diode of 10 cm^{-1} at the hot and cold wavelength is assumed. For simplicity, a linear model

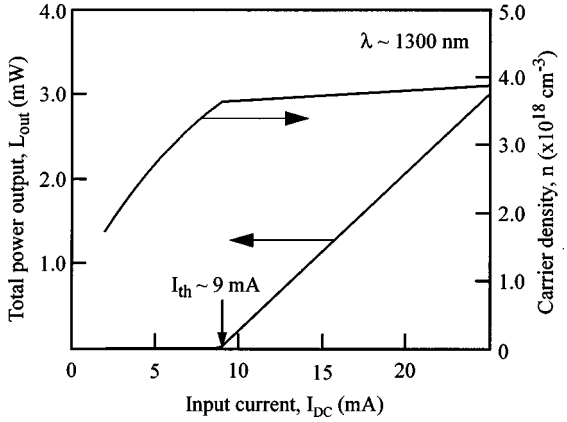

FIG. 5. Calculated steady-state L_{out}–I_{DC} and $n-I_{DC}$ for the multi-cavity laser used in our study and as in Fig. 1. The presence of homogeneous gain compression, $\epsilon=2\times10^{-17}$ cm^3 leads to a lack of carrier pinning above I_{th}.

of the gain, $G=\Gamma v_g g_{slope}(n-n_0)$, is used in our analysis with a gain slope of $g_{slope}=4.4\times10^{-16}$ cm^2 at λ_{COLD}, $g_{slope}=4.7\times10^{-16}$ cm^2 at λ_{HOT}, and transparency carrier density for both wavelengths of $n_0=2.5\times10^{18}$ cm^{-3}. (We note, for the more complex set of parameters $g_{slope}(\lambda_{COLD})=4.7\times10^{-16}$ cm^{-2}, $n_0(\lambda_{COLD})=2.57\times10^{18}$ cm^{-3}, $g_{slope}(\lambda_{HOT})=4.4\times10^{-16}$ cm^{-2}, and $n_0(\lambda_{HOT})=2.41\times10^{18}$ cm^{-3}, essentially identical results are obtained.) A mode confinement factor $\Gamma=0.1$ is used for both wavelengths. Homogeneous gain compression of 2×10^{-17} cm^3 and a spontaneous emission factor of $\beta=10^{-4}$ at both the wavelengths is assumed. The values chosen are typical of 1.3 μm InGaAsP lasers[8] and we assume that λ_{HOT} and λ_{COLD} are approximately 1.3 μm with about 10 nm spectral separation. The gain slopes at λ_{HOT} and λ_{COLD} and the reflectivity of the gratings are the parameters tailored to fit measured data such as threshold current and mode suppression.

Figure 5 shows the calculated steady state light output versus current (L_{out}–I_{DC}) and the carrier density versus current ($n-I_{DC}$) for the laser. A threshold current, $I_{th}\sim9$ mA is seen from the L_{out}–I_{DC} characteristics which match that of the experimental device. The predicted lack of carrier pinning above laser threshold current is due to gain compression.

Figure 6(a) shows the rectifying action of the laser diode on rf current flow. After time $t=0$, the sinusoid current amplitude is $I_{RF}=3\times I_{th}$ superimposed on a steady-state current $I_{DC}=18$ mA. In the model, only positive current flows through the diode. Shown in Figs. 6(b) and 6(c) is the calculated temporal evolution of wavelength switching in the multi-cavity laser due to a rf signal tuned to the cold cavity resonance. The rf signal drives the laser below threshold during portions of the negative half cycle and hence causes gain switching to occur. Since the rf signal is tuned to the cold cavity resonance, the average dynamic gain seen by the cold wavelength is larger than that seen by the hot wavelength. Hence, the lasing wavelength changes from the hot wavelength to the cold wavelength. Figure 6(c) shows that about 7–8 photon-cavity round-trips are needed to switch to the cold wavelength. The transient switching time is determined

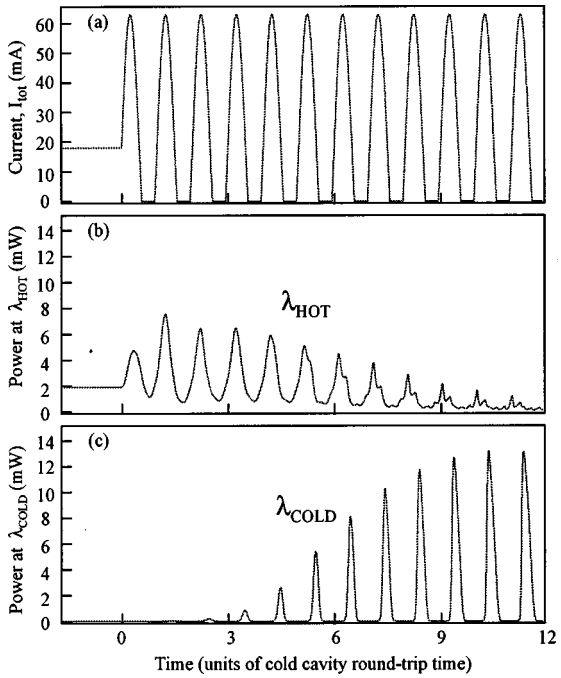

FIG. 6. Transient switching response when a rf signal tuned to the cold cavity resonance is turned on; (a) total current, I_{tot}, input to the laser, with $I_{DC}=2\times I_{th}$ and $I_{RF}=3\times I_{th}$, (b) the response of the hot photons, (c) pulse buildup dynamics of the cold photons. It takes about seven round-trips for the cold wavelength to build up and reach 50% of the steady-state intensity.

by the relative dynamic gain at each wavelength and the fact that photons at the hot wavelength must first be reduced before increasing the number of photons at the cold wavelength. There are some spikelike features in the optical power output at the hot wavelength even after the average value has been suppressed. This is due to the difference in the round-trip times for the hot and cold photons which affect each other directly through gain compression and indirectly through carrier density variation.

Figure 7 shows the effect of bias current I_{DC} and the rf current I_{RF} on the calculated rise time for hot and cold switching. It is of interest to note that switching to the cold wavelength takes longer than switching to the hot wavelength. This is because hot photons in the cavity must first be suppressed before significant buildup of the cold photons. Further, the trends shown here agree qualitatively with the experimental results shown in Fig. 4. The only discrepancy is in the case of switching to λ_{COLD} for a given rf current, I_{RF}, as the bias current I_{DC} is increased above threshold. In this situation, the numerical results indicate that the switching time should increase with an increase in the bias current I_{DC} while the experimental results show that it is independent of the bias current. Naively, one expects the number of hot photons in the cavity to affect the switching transients and they increase with I_{DC}. Hence, we expect our simulations to show an increase in the cold switching time with an increase in I_{DC} above threshold. Our numerical simulations show this result but the experiments do not. We tentatively ascribe the discrepancy to the simplistic model used which does not take into account the effects of modelocking and the residual reflectivity of the AR coated facet.[4]

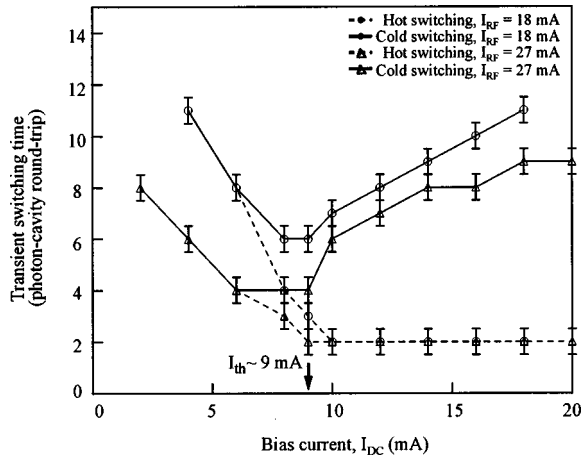

FIG. 7. Transient switching time for cold cavity switching (solid curve) and hot cavity switching (dashed curve), as a function of the bias current, I_{DC}, for the different indicated rf currents, I_{RF}. Note that the rf source is a voltage source capable of supplying the indicated maximum current. However, the total current $I_{tot}=[(I_{DC}+I_{RF}\sin(2\pi f_{RF}t)]$ into the laser is always non-negative at any time instant. If I_{tot} becomes negative, the current into the laser is clamped to zero. The error bars in the figure are due to an uncertainty of a round-trip in the rise time.

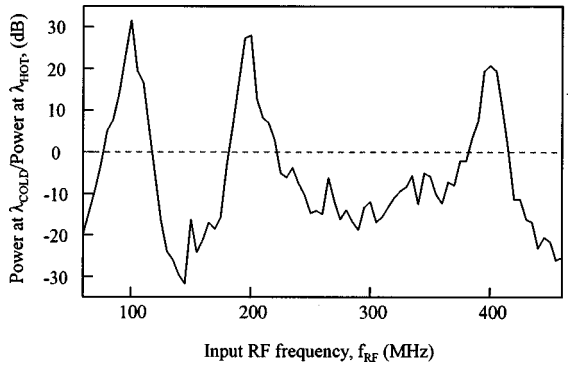

FIG. 8. Ratio of the average power in the cold wavelength to that in the hot wavelength (mode suppression ratio) as a function of the input rf frequency for a fixed bias current, $I_{DC}=2\times I_{th}$ and rf excitation, $I_{RF}=3\times I_{th}$. The cavity lengths are increased so that the fundamental cavity resonant frequencies are $f'_{COLD}=100$ MHz and $f'_{HOT}=150$ MHz. A large value indicates good wavelength switching. The presence of switching at higher harmonics and a lack of switching at 300 MHz is clearly seen. The dashed line indicates the case when the hot power is equal to the cold power.

As shown in Fig. 7, the cold switching time decreases with an increase in rf current independent of the bias current. This is to be expected since rf modulation decreases the effective dynamic loss seen at the cold wavelength compared to the hot wavelength. For the hot switching time, an increase in the rf modulation causes a faster turn-on when biased below threshold since this decreases the effective dynamic loss at the hot wavelength. However, when the laser is biased above threshold, this effect is negligible since the device is already lasing and has hot photons in the cavity. Hence, the hot switching time is independent of the rf power when biased above threshold. An analogy would be the almost negligible dependence of the turn-on delay of an above threshold (on–on) modulated laser on the modulation depth. Intuitively, we expect the time taken to switch to λ_{COLD} to decrease when the spectral separation between λ_{HOT} and λ_{COLD} is decreased. This is confirmed by our simulations whose results (not shown in figure) indicate a decrease of two round-trips in the rise time for switching to λ_{COLD}, independent of the bias current I_{DC}, when the differential gain at λ_{COLD} is increased by approximately 2%. Hence, the transients are determined by the relative values of the dynamic gain and loss at both wavelengths.

We also investigated the possibility of switching the cavity using harmonics of the fundamental cavity resonant frequency. The external cavity length is increased so that the fundamental cavity resonant frequencies are $f'_{COLD}=100$ MHz and $f'_{HOT}=150$ MHz. We define mode suppression ratio as the steady-state ratio of the time averaged optical power at the cold wavelength to that at the hot wavelength and use it as a quantitative measure of the effectiveness of switching. Shown in Fig. 8 is the calculated dependence of the optical mode suppression ratio [power (λ_{COLD})/power(λ_{HOT})] on the RF input signal frequency. From Fig. 8 we find that switching to the cold wavelength is possible at higher harmonics. We also find that switching using the third harmonic is not possible. This is because the second harmonic of the hot cavity (2×150 MHz$=300$ MHz) matches the third harmonic of the cold cavity (3×100 MHz $=300$ MHz). Hence, if an rf signal at 300 MHz is applied, the hot cavity photons are not suppressed and wavelength switching is not feasible at this frequency. A similar lack of switching is also seen at 600 MHz (not shown in Fig. 8) when the $m=6$ harmonic of f'_{COLD} and $n=4$ harmonic of f'_{HOT} coincide. Further, it is of interest to note that the mode suppression ratio at 300 MHz (~-20 dB) is not as impressive as that at 150 MHz (~-33 dB). We attribute this to an increase in the large signal gain at λ_{COLD} due to the cold cavity round-trip resonance at 300 MHz ($=3\times f'_{COLD}$). As expected, lasing occurs at the hot wavelength when excited by an rf frequency that does not match the fundamental or a harmonic of the cold cavity resonance frequency, f'_{COLD}. The rf bandwidth of the resonance is determined by the temporal shape and duty cycle of the electrical pulse-train used to gain switch the laser. Simulations give 40 MHz of rf bandwidth for switching to λ_{COLD} which should be compared with the measured value of 100 MHz. It is interesting to note that when the applied rf signal does not match either the fundamental or harmonic of either f'_{COLD} or f'_{HOT}, the gain switched pulse of photons after a round-trip will not be in synchrony with the current excitation. However, due to the large duty cycle of the pulse, some photons from the partially quenched media see a large gain and are amplified. Due to experimental limitations such as the relative locations of the gratings in the fiber Bragg grating and the frequency response of the laser diode used, we did not attempt to experimentally measure switching using higher harmonics.

III. WAVELENGTH SWITCHING USING LIGHT INJECTION

A. Model and results of numerical simulation

When cavity lengths are scaled so that the fundamental cavity resonant frequencies are greater than 10 GHz, it becomes increasingly difficult to couple the rf excitation

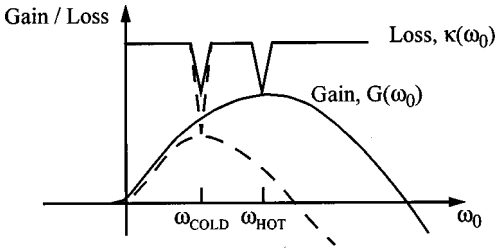

FIG. 9. Schematic showing the gain and effective loss vs optical frequency, ω_0. The dashed curves show that the effective loss at λ_{COLD} is decreased by coherent light injection at that wavelength causing the laser to switch the lasing wavelength and change the gain spectrum.

needed to effect wavelength switching. This is due to the junction capacitance of the laser and other rf parasitics. Hence, the technique of optical wavelength switching using an rf signal is not suitable for short cavities. Another method of wavelength switching uses injection of lasing light into the multi-cavity device. As shown schematically in Fig. 9, the dynamics of such all-optical switching is determined by modulation of effective photon lifetimes in the cavity.

We use the model described earlier in this article with the boundary condition for the cold wavelength at the non-AR coated facet modified from Eq. (6) to

$$S^{+}(0;t;\lambda_{COLD}) = R_1 \times S^{-}(0;t;\lambda_{COLD}) + S_{inj} + k\sqrt{S_{inj} \times R_1 \times S^{-}(0;t;\lambda_{COLD})}, \tag{7}$$

where S_{inj} is the number of photons injected into the cavity from the non-AR coated facet side. The square-root term takes into account interference from the coherent addition of the electric fields. For the sake of simplicity, the constant k in the equation is set equal to unity. The laser parameters used in the model are as described in Sec. II B. If the active region is excited by a constant current $I_{DC} > I_{th}$, the output of the laser is photons at the hot wavelength when $S_{inj} = 0$. However, when photons at the cold wavelength are step injected as shown in Fig. 10(a) (200 μW optical power shown as solid line, 100 μW broken line), the average carrier density in the semiconductor changes as shown in Fig. 10(b) and wavelength switching shown in Figs. 10(c)–10(d) occurs. The injection of cold photons alters the effective photon lifetime (optical loss) and thereby causes wavelength switching. This is confirmed by the fact that the average carrier density decreases after the laser switches to λ_{COLD}. The presence of steps in intensity every round-trip time is a signature of external cavity photon intensity buildup[1,2] and is clearly seen in Figs. 10(c)–10(d).

It is of interest to note that the 50% rise time using optical injection to switch to the cold wavelength is only 2–3 round-trips which is better than ~8 round-trips needed using the rf method described in Sec. II. This difference exists even though ~10 mW power is injected using the rf method compared to ~0.1 mW power for the optical method. The reason for this is that optical injection alters the photon lifetime almost instantaneously, while the rf method alters the effective dynamic loss $K_{eff}(f_{RF}, \omega_0)$ via the carrier density. In addition, optical injection seeds the buildup of cavity photons, whereas in the rf method the small number of photons at λ_{COLD} have to act as the photon seed. Hence, the rf method of wavelength switching is inherently slower and less efficient than the optical injection method.

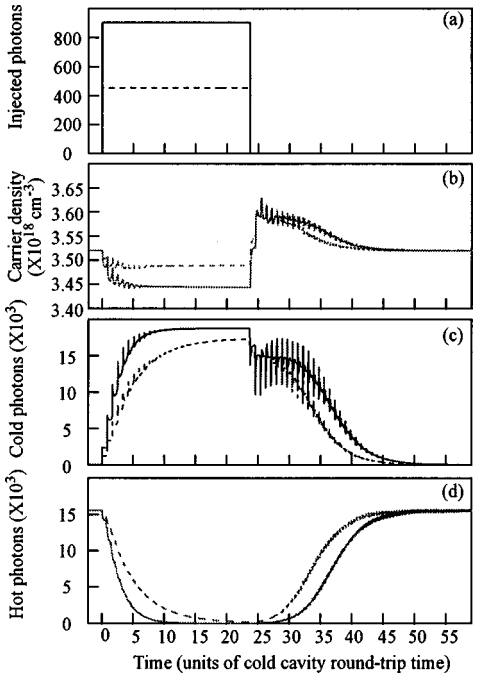

FIG. 10. The transient switching response when a fixed number of cold photons are continuously injected into the lasing region. The laser is biased at I_{DC}=18 mA and the threshold current I_{th}=9 mA with a light output of ~1.75 mW from the non-AR coated facet before cold photons are injected. The broken curves correspond to a smaller photon injection and the solid curves for the larger photon injection. (a) The number of cold photons injected into the cavity (~200 μW for the solid curve and ~100 μW for the broken curve) to effect wavelength switching. (b) The temporal response of the average carrier density within the semiconductor region during wavelength switching. (c) The dynamics of the buildup/decay of the total number of cold photons in the cavity during wavelength switching. (d) The total number of hot photons in the cavity as a function of time.

After photon injection is turned off, we see from Fig. 10 that the laser switches back to lasing at λ_{HOT} and S_{COLD} decreases. The ringing in S_{HOT} after switching back to lasing at λ_{HOT} is due to the presence of an external cavity and the ringing decays away after a few round-trips. It is of interest to note that this switching back to λ_{HOT} takes 10–13 round-trips. Switching from λ_{COLD} to λ_{HOT} consists of two regimes; regime (i) consisting of approximately 1 round-trip after turning off light injection; regime (ii) consists of about 9–12 round-trips after regime (i). During regime (i), the average carrier density in the active region increases to a value so as to sustain laser oscillation at λ_{COLD}. This increase in the carrier density is accounted for by a decrease in the number of cold photons in the cavity. However, the laser is still lasing at λ_{COLD} but with fewer number of cold cavity photons. Regime (ii) consists of the buildup of hot photons and the decay of cold photons and carriers to the value present before any light injection. This is analogous to the case when the laser switches from lasing at λ_{HOT} to λ_{COLD}. However, it takes longer to switch back to λ_{HOT} because the number of hot (seed) photons present in the cavity just before turning off photon injection is very small.

The effect of decreasing the photon injection power on the switching transients can also be seen from Fig. 10 (dashed curves). Decreasing the photon injection causes a decrease in the change in effective cold-photon lifetime (i.e., decrease in the difference between effective cold-photon lifetime and hot-photon lifetime). This causes the rise time to increase (~2 round-trips) and the number of cold photons to decrease. The time needed to switch back to λ_{HOT} after a lower light injection is turned off is smaller (~10 round-trips). This is due to an increase in the number of hot photons present, just before turning off light injection. From Fig. 10 it is clearly seen that the transients are determined by the change in effective photon lifetimes. Further, when λ_{COLD} is moved closer in wavelength towards λ_{HOT}, the accompanying increase in the differential gain at λ_{COLD} causes the switching to λ_{COLD} (with photon injection) to be faster and subsequently, with the turning off of photon injection, switching back to lasing at λ_{HOT} takes a longer time (not shown in Fig. 10). There is a finite time to switch to λ_{COLD} which can be reduced to almost one photon-cavity round-trip by increasing photon injection intensity or placing the two wavelengths closer to each other spectrally. The disadvantage of such an approach is that the time taken to switch back to λ_{HOT} increases and the mode suppression ratio decreases. At this bias, a minimum photon injection power of 50 μW at λ_{COLD} is needed to switch to λ_{COLD} with 10 dB mode suppression ratio (not shown in the figure).

Although our model ignores mode pulling due to injection locking, bistability, hysteresis, etc., it nonetheless predicts qualitatively behavior which was subsequently observed experimentally.

C. Experimental arrangement and experimental results

A schematic diagram of the experimental arrangement is shown in Fig. 11(a). The laser used for the experiments on cavity switching using optical injection is the same as that described in Sec. II A. The AR coated laser emitting at 1.3 μm obtains optical feedback from two Bragg gratings with center wavelengths λ_{HOT}=1312 nm (λ_{COLD}=1309 nm) embedded in a lensed SMF approximately 80 cm from the lensed end. The 2 mm long Bragg gratings are spaced 1 cm apart. The photon-cavity round-trip time is ~8 ns. The coupling efficiency between the AR coated laser and the lensed fiber with the embedded Bragg gratings is adjusted so that the device lases at wavelength λ_{HOT}.[9] The laser has a threshold current of 14 mA in the external cavity.

A tunable laser is obtained by placing another AR coated laser emitting at 1.3 μm in an external cavity with optical feedback from a bulk diffraction grating. The light output of the tunable laser is collected from the cleaved facet using a lensed SMF. The light is then passed through an optical isolator and a lithium niobate switch before it is injected into the multi-cavity laser at the cleaved facet (non-AR coated facet). The light output from the SMF containing the Bragg gratings is collected at the detector.

Figures 11(b)–11(d) show experimental results of wavelength switching using an optical input. When no light is injected into the semiconductor laser the laser lases at λ_{HOT}.

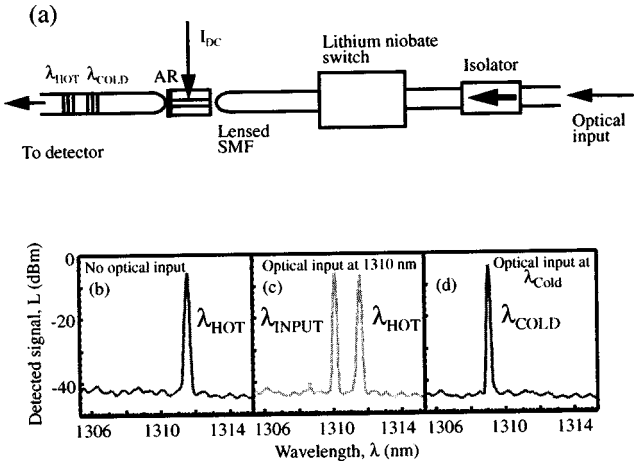

FIG. 11. (a) A schematic diagram of the experimental arrangement. The AR coated laser emitting at 1.3 μm obtains optical feedback from two Bragg gratings with center wavelengths λ_{HOT}=1312 nm (λ_{COLD}=1309 nm) embedded in a SMF. The laser has a threshold current I_{th}=14 mA in the external cavity. The optical input injected into the laser is obtained from a tunable laser. The optical spectrum of the light output of the multi-cavity laser when (b) no light is injected, (c) injected light is neither at λ_{HOT} nor λ_{COLD}, and (d) injected light is at λ_{COLD}.

If light is injected into the semiconductor laser at a wavelength, λ_{INPUT} (other than λ_{HOT} or λ_{COLD}) the light output has a component at λ_{INPUT} and at λ_{HOT}. When light at λ_{COLD} is injected into the device laser output switches to λ_{COLD}. Further, at a light output power level of 1 mW, a minimum photon injection power of 200 μW at λ_{COLD} ensures wavelength switching with 30 dB mode suppression.

Shown in Fig. 12(a) are measured transients for switching to the cold wavelength, λ_{COLD}, due to injection of light at the cold wavelength. The amount of power injected is estimated to be approximately 200 μW and the laser is biased at I_{DC}=18 mA. We see that the time taken to reach 50% of the steady-state value is less than two photon-cavity round-trip times which is similar to the value obtained earlier with our numerical simulations. Shown in Fig. 12(b) is the measured transient to switch back to the hot wavelength after the light injection is turned off. It takes several (~20) round-trips to reach steady state lasing at λ_{HOT}. Further, it is interesting to note the presence of a ''shoulder'' in the decrease of cold photon intensity. This is as predicted by our numerical simulations and is attributed to the two regimes involved in the transients. In the first regime the carrier density increases at the expense of cold photons to maintain lasing at the cold wavelength. This occurs during the first couple of round-trips after light injection is turned off. In the second regime hot photons in the cavity build up at the expense of cold photons and carrier density. The carrier density then decays to a value such that it supports lasing at λ_{HOT}.

The method outlined above is an extension of the injection locking concept[10] to multi-cavity lasers to effect wavelength switching. Further, this method of wavelength switching is not necessarily limited to multi-cavity lasers. It can also be used to switch wavelength in novel microlasers, where the external cavity lengths are reduced essentially to zero.

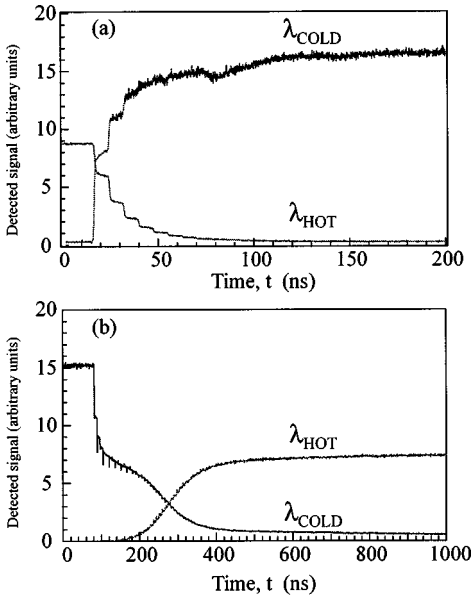

FIG. 12. The transient switching response obtained experimentally when light at wavelength λ_{COLD} is injected into the cavity. The device is biased at $I_{DC}=18$ mA which is slightly above the threshold current $I_{th}=14$ mA. The output of the laser at this bias current before any optical injection is ~150 μW. We estimate that about 200 μW (a fraction of which is at the correct polarization) at λ_{COLD} is injected into the laser. The photon-cavity round-trip time is ~8 ns for both λ_{HOT} and λ_{COLD}. (a) The transients involved in switching to λ_{COLD} with the injection of light. (b) Temporal response involved in switching back to λ_{HOT} when the light injection is turned off.

IV. CONCLUSION

In conclusion, transient wavelength switching induced by rf modulation of multi-cavity laser diodes has been numerically simulated and compared with experimental results. Ultrafast hot cavity switching is possible. In this situation only 1.5 photon-cavity round-trip times are required to switch wavelength. However, cold cavity switching requires a total of 8 round-trip times of which 5–6 round-trips are used to suppress lasing intensity at wavelength λ_{HOT} before intensity at λ_{COLD} begins to increase.

Our numerical simulations indicate and experimental results show that injection of coherent light into a nonlasing optical mode may also be used to switch lasing wavelength. In this situation there is a significant asymmetry between the λ_{HOT} and λ_{COLD} transient (2–4 round-trips) and the λ_{COLD} to λ_{HOT} transient (10–13 round-trips). Applications of all-optical wavelength switching will be limited by the time taken to switch back to λ_{HOT} after turning off light injection. Transient switching times can be decreased by choosing wavelengths which optimize dynamic gain and loss values. Our work shows that the initial number of photons present in a nonlasing mode influences the switching speed to that mode at the expense of mode suppression ratio. However, the need for significant mode suppression ratios in practical systems will force a reduction in maximum achievable switching speed.

This technique of wavelength switching using light injection will find use in high-speed, small cavity, high-Q microlasers. Further, one can envision very high Q microlasers such as whispering gallery mode lasers wherein optical wavelength switching occurs in a few picoseconds. The use of novel scaled devices that may change the direction of light output by injecting light into a nonlasing spatial mode is also a possibility.

ACKNOWLEDGMENTS

This work is supported in part by Joint Services Electronics Program under Contract No. F49620-94-0022, and the Air Force Office of Scientific Research under Contract Nos. F49620-96-1-0357 and F49620-97-1-0438.

[1] N. A. Olsson and W. T. Tsang, IEEE J. Quantum Electron. **QE-19**, 1479 (1983).
[2] J. O'Gorman, A. F. J. Levi, D. Coblentz, T. Tanbun-Ek, and R. A. Logan, Appl. Phys. Lett. **61**, 889 (1992).
[3] D. Huhse, M. Schell, W. Utz, D. Bimberg, J. A. R. Williams, L. Zhang, and I. Bennion, Appl. Phys. Lett. **69**, 2018 (1996).
[4] A. P. Kanjamala and A. F. J. Levi, Appl. Phys. Lett. **69**, 3647 (1996).
[5] K. Kojima, Optical Fiber Communications Conference, 1995, OSA Technical Digest Series, ISBN 1-55752-368-1, Vol. 8, p. 253.
[6] A. P. Kanjamala, Ph.D. dissertation, University of Southern California, 1998.
[7] J. E. Bowers, P. A. Morton, A. Mar, and S. W. Corzine, IEEE J. Quantum Electron. **QE-25**, 1426 (1989).
[8] G. P. Agrawal and N. K. Dutta, *Semiconductor Lasers*, 2nd ed. (Van Nostrand Reinhold, New York, 1993).
[9] A. P. Kanjamala and A. F. J. Levi, Appl. Phys. Lett. **71**, 300 (1997).
[10] R. Lang, IEEE J. Quantum Electron. **QE-18**, 976 (1982).